CHD4-NURD controls spermatogonia survival and differentiation

Rodrigo O. de Castro[*], Victor Goitea[*], Luciana Previato[*], Agustin Carbajal[*], Courtney T. Griffin[†,‡], and Roberto J. Pezza[*,‡,§].

[*]Cell Cycle and Cancer Biology Research Program, Oklahoma Medical Research Foundation, Oklahoma City, Oklahoma, United States of America.

[†]Cardiovascular Biology Research Program, Oklahoma Medical Research Foundation, Oklahoma City, Oklahoma, United States of America.

[‡]Department of Cell Biology, University of Oklahoma Health Science Center, Oklahoma City, Oklahoma, United States of America.

[§]Corresponding author: Roberto J. Pezza. Suite B305. 825 NE 13th street, Oklahoma City, Oklahoma, 73104. Tel. 405-271-6467. Email: pezzar@omrf.org.

Running title: CHD4-NURD function in gametogenesis

Key words: mouse gametogenesis, spermatogonia, NURD, and testis development.

Abstract

Testis development and sustained germ cell production in adults rely on the establishment of spermatogonia stem cells and their proper differentiation into mature gametes. Control of these processes involves not only promoting the expression of genes required for cell

survival and differentiation but also repressing other cell fates. This level of transcriptional control requires chromatin-remodeling complexes that restrict or promote transcription machinery. Here, we investigated the roles of the **NU**cleosome **R**emodeling and **D**eacetylase (NURD) complex during spermatogenesis. Our cytological and biochemical analyses revealed differential expression and composition of NURD subunits in gametocytes at different stages of testis development. Germ cell-specific deletion of the NURD catalytic component CHD4, but not CHD3, resulted in male infertility due to failed maintenance of the undifferentiated spermatogonia stem cell population. Genome-wide CHD4 localization and transcriptomic analyses revealed that CHD4 binds the promoters and regulates the expression of genes involved in spermatogonia cell survival, and differentiation. These results uncover the requirements of CHD4 in mammalian gonad development, and point to unique roles for the NURD complex with respect to other chromatin remodelers during gamete development.

Significance Statement

Gametogenesis is a fundamental developmental program required for sustained fertility and survival of all sexually reproducing species. The developing male gamete undergoes numerous cell divisions and developmental stage transitions that are carefully monitored by epigenetic mechanisms. One prominent mechanism is directed by chromatin remodeling complexes, which modify chromatin structure and thereby control fundamental cellular processes such as gene transcription. In this work, we focused in understanding the role of CHD4 and CHD3 proteins, catalytic subunits of the NURD chromatin-remodeling complex, in mouse gametogenesis. We find that CHD4 has an essential function in gametogenesis, with an absolute requirement for maintenance of and differentiation of spermatogonia populations in the developing testis. This is achieved by

CHD4-mediated transcriptional regulation of genes important for spermatogonia survival, and differentiation.

Introduction

Defects in gametogenesis are a leading cause of infertility and an important cause of birth defects associated with aneuploidy. Insights into the mechanisms underlying testis formation, including spermatogonia stem cell and spermatocyte development, are necessary to improve the outcomes of common gonad developmental diseases.

In mice, spermatogenesis begins from isolated germ cells called spermatogonia singles (A_s) that undergo to a series mitotic divisions with incomplete cytokinesis, to produce spermatogonia stem/progenitor cells (SPCs) known as paired (A_{pr}) and aligned ($A_{al\text{-}4\ to\ 16}$). The stem cells activity is lost during the transition from A_{al} to A1. At this point, spermatogonia cells start a process of differentiation (A1, A2, A3, A4 or intermediate (In), formation of type B spermatogonia, and then transition to pre-leptotene cells that initiate the series of meiotic divisions that ultimately originate spermatozoa.

Chromatin undergoes extensive remodeling during gametogenesis, leading to altered gene expression and chromosome organization, and ultimately controlling obligatory developmental transitions such as the conversion from undifferentiated to differentiated spermatogonia type and spermatogonia commitment to meiosis (1, 2). The NURD (NUcleosome Remodeling and Deacetylase) complex is a prominent chromatin modifying complex that functions to repress target gene expression via chromatin remodeling and histone deacetylation (3, 4). The NURD complex contains two highly conserved and widely expressed catalytic subunits, CHD3/Mi-2α (chromodomain-helicase-DNA-binding 3) and CHD4/Mi-2β, which are members of the SNF2 superfamily of ATPases (3-7). NURD plays a central role in various developmental and cellular events, such as controlling the

differentiation of stem cells, maintaining cell identity, and responding to DNA damage (7-9). However, its role in gamete development has not been yet defined and no studies to date have addressed the requirements or mechanisms of CHD4 and CHD3 in any gametocyte type.

In this study, we report that CHD4 (but not CHD3) is essential for testis development and sustained germ cell production in adults. Germ cell-specific deletion of CHD4 results in the developmental arrest of undifferentiated spermatogonia. Our system-wide analysis of CHD4 target genes and transcriptional profiling suggest that CHD4 contributes to early germ cell development by regulating the transcription of specific genes that are important for survival and differentiation of spermatogonia cells. This study defines molecular and cellular mechanisms for CHD4 and the NURD complex in regulating gamete development.

Results

Chd4 expression during mouse germ cell development

To investigate a potential role for CHD4 in germ cells, we assessed CHD4 expression in newborn and adult mouse testes by immunofluorescence. CHD4 was highly expressed in the nuclei of spermatogonia cells (marked by PLZF, aka ZBT16) and in Sertoli cells (marked by SOX9) (Fig. 1A and Fig. S1), but not in the negative control (PLZF-positive spermatogonia from *Chd4*$^{-/-}$ testes, Fig. S2A). PLZF is expressed from A_s to A1(10, 11). The nuclear immunosignal of CHD4 was diminished in cells undergoing the first meiotic division (i.e. zygotene-pachytene) (Fig. 1B). In agreement with a previous report (9, 12-16), we also observed CHD4 immunostaining at the chromosomal sex body in pachytene spermatocytes (Fig. 1B-b). In sum, CHD4 is highly expressed in spermatogonia with

prominent nuclear localization, suggesting a role for CHD4 in early events of male gametogenesis.

We confirmed that CHD4 is expressed at both pre-meiotic and meiotic stages of male gamete development by analyzing CHD4 protein levels in enriched fractions (see methods for details) of undifferentiated and differentiating spermatogonia (obtained from wild type 7dpp mice and using THY1.2+ and c-KIT+ affinity columns, respectively), Sertoli cells, and pachytene spermatocytes (Fig. 1C). The level of cell population enrichment was assessed by western blot and markers specific for Sertoli (SOX9), differentiating spermatogonia (STRA8), and primary spermatocytes (SYCP3) (Fig. 1C and S2B).

Composition of CHD4-NURD complexes during spermatogenesis

NURD function is influenced by its subunit composition(17). To determine whether the expression of NURD composition might change during spermatogenesis, first we analyzed the levels of representative NURD subunits in enriched fractions of undifferentiated and differentiating spermatogonia, Sertoli cells, and pachytene spermatocytes. Similar to CHD4, the NURD subunits HDAC2, MTA1, RBBP4, RBBP7 and MBD2 were present in enriched fractions of undifferentiated (THY1.2+) and differentiating (c-KIT+) spermatogonia (Fig. 1C). The levels of MTA, RBBP7, and MBD2 subunits were substantially reduced or absent in pachytene spermatocytes, suggesting a particular composition and perhaps a different function for CHD4-NURD in this cell type.

To determine the composition of CHD4-NURD complexes, we used co-immunoprecipitation analysis to uncover NURD subunits that interact with CHD4 in enriched fractions of Sertoli and spermatogonia cells. The NURD subunits HDAC2A, MTA1, and RBBP4, but not MBD2, coimmunoprecipitated with CHD4 from Sertoli and Spermatogonia cells (Fig. 1D). HDAC2A, but not CHD3, coimmunoprecipitated with CHD4 from wild type and *Chd3*$^{-/-}$ spermatogonia cells (Fig. S2C). These data suggest that: i)

CHD4 forms a NURD complex independently of CHD3, ii) CHD3 and CHD4 occupancy within the NURD complex is mutually exclusive, and iii) that loss of CHD3 does not perturb CHD4-NURD complex formation in spermatogonia cells.

Our results suggest that a CHD4-NURD complex composed of CHD4, HDAC2A, MTA1 and RBBP4 functions in mouse spermatogonia and Sertoli cells.

Deletion of *Chd4* but not *Chd3* results in testis developmental defects

To examine the potential functions of *Chd4* and *Chd3* during spermatogenesis, we generated a series of *Chd4* and *Chd3* germline conditional knockout mice (Fig. 2A-C). To delete the floxed allele in primordial germ cells (embryonic day 15.5, Fig. 2C) (18, 19), male Ddx4-Cre; $Chd4^{WT/\Delta}$ were crossed with $Chd4^{fl/fl}$ females to generate Ddx4-Cre; $Chd4^{fl/\Delta}$ conditional knockout mice (here called Ddx4-$Chd4^{-/-}$). A similar strategy was used to generate Ddx4-$Chd3^{-/-}$ mice (Fig. 2B), as well as Spo11-$Chd4^{-/-}$ mice, which delete the floxed allele only in early primary spermatocytes (Fig. 2C) (20). We confirmed deletion of *Chd3* and *Chd4* by RT-qPCR (Fig. 2D).

Ddx4-$Chd4^{-/-}$ adult mice (2 months old) appeared normal in all aspects except in the reproductive tissues. Testes were significantly smaller in Ddx4-$Chd4^{-/-}$ males (mean: 0.017g ± SD: 0.005, n=4, P≤0.0001, t test) compared to wild type (0.104 g ± 0.005, n=6) littermates (Fig. 2E), indicating severe developmental defects in the testis. In contrast, Spo11-$Chd4^{-/-}$ (0.096g ± 0.011, n=3; P=0.21, t test), and Ddx4-$Chd3^{-/-}$ males (0.095g ± 0.002, n=3, P=0.04, t test) did not show any significant difference in testis size compared to wild type littermates (Fig. 2E). Thus, CHD4, but not CHD3, plays an important role in mouse male gametogenesis. Moreover, the normal testis size of Spo11-$Chd4^{-/-}$ mice suggests that developmental defects triggered by CHD4 depletion originate in pre-meiotic stages of gamete development.

We found that Ddx4-*Chd4*$^{-/-}$ males develop testicular hypoplasia with hyperplasia of interstitial cells and lack spermatozoa, with Ddx4-*Chd4*$^{-/-}$ showing a more severe phenotype (Fig. 3A). The number of seminiferous tubules is similar between wild type and mutant animals, but the diameter is reduced (wild type, mean ± SD, 287 ± 34, n=400 seminiferous tubules cross sections (3 different mice) versus *Chd4*$^{-/-}$ 148 ± 21.3, n=210, P<0.0001 t test).

Analysis of Ddx4-*Chd4*$^{-/-}$ testes revealed a total loss of germ cells (marked by TRA98) in seminiferous tubules (Fig. 3B). No developing gametes were observed, including cell types at early stages (e.g. spermatogonia) (Fig. 3 A and B). Sertoli cells develop normally in Ddx4-*Chd4*$^{-/-}$ mice, consistent with the specific loss of *Chd4* in germ cells at early stages of development. We did not observe differences in germ cell development between wild type and Ddx4-*Chd3*$^{-/-}$ or Spo11-*Chd4*$^{-/-}$ mice (Fig. S3B and C), consistent with their similar testes sizes (Fig. 2).

We also analyzed H&E stained histological sections of ovaries from 45-day-old wild type and Ddx4-*Chd4*$^{-/-}$ female mice. We noted a significant reduction in ovary size, an increase in stromal cells, a reduced number of follicles (wild type, 10 ± 3, n=6 mice versus Ddx4-*Chd4*$^{-/-}$ 0.6 ± 0.9, n=5, P<0.0001 t test) and a reduced number of corpora lutea (wild type, 9 ± 1, n=6 mice versus Ddx4-*Chd4*$^{-/-}$ 0 ± 0, n=5, P<0.0001 t test) in the Ddx4-*Chd4*$^{-/-}$ mice compared to wild type (Fig. 3C).

We conclude that deletion of *Chd3* has apparent no effect on gamete development. However, germ cell specific deletion of *Chd4* results in severe male and female germ cell developmental defects, possibly originated at premeiotic stages of development.

CHD4 is dispensable for mouse meiosis

CHD4 is known to play a role in the DNA damage response (reviewed in (21)). For example, *Chd4* knockdown results in increased γH2AX, a marker of double-strand breaks,

and CHD4 accumulates at sites of DNA damage (2). To determine whether CHD4 is required to repair the programmed double-strand breaks that occur in gametocytes during meiosis, we immunostained spermatocyte chromosome spreads for γH2AX and RAD51, markers of DNA repair and recombination. In agreement with the normal development and cellular composition of Spo11-*Chd4*$^{-/-}$ testes (Fig. S3C), the kinetics of formation and repair of double-stand breaks appeared normal in Spo11-*Chd4*$^{-/-}$ mice (Fig. S4). Further, chromosome pairing and synapsis in Spo11-*Chd4*$^{-/-}$ spermatocytes was indistinguishable from wild type cells.

We conclude that CHD4 is dispensable for proper repair of double-stand breaks and homologous chromosome interactions in mouse spermatocytes and for progression of meiosis in the mouse.

CHD4 is required for spermatogonia survival

The severe phenotypes observed in Ddx4-*Chd4*$^{-/-}$ mice (Fig. 2 and 3) prompted us to investigate spermatogonial differentiation during testis development in newborns. Testis sections from 9 dpp Ddx4-*Chd4*$^{-/-}$ mice stained with H&E showed a markedly reduced number of gametocytes, as well as differences in cell composition, compared to those from age-matched wild type mice (Fig. 4A, a and b). To analyze this in detail, we examined the expression of TRA98 and STRA8, which mark germ cells and differentiating spermatogonia, respectively. Whereas tubules from 9 dpp wild type mice contained cells expressing TRA98 (35 ± 9.8, n=22) and STRA8 (18.8 ± 8.4, n=36), tubules from *Chd4*$^{-/-}$ mice showed a near absence of cells expressing these markers (TRA98, 4.6 ± 3.1, n=20. STRA8 2.5 ± 3.5, n=42) (Fig. 4A, c-f). Testes sections from 9 dpp *Chd4*$^{-/-}$ mice also showed a reduction in primary spermatocytes expressing the meiotic prophase I markers SYCP3 and γH2AX compared to those from 9 dpp wild type mice (Fig. S5A and B).

Together, the results further suggest that testis defects in *Chd4*$^{-/-}$ mice begin early, during pre-meiotic stages of postnatal development, leading to an absence of germ cells in adults.

To pinpoint when and where the testes defects originate in *Chd4*$^{-/-}$ mice, we compared the number of PLZF positive cells (which marks single, paired, and aligned spermatogonia) in 4dpp whole-mount tubules obtained from wild type and *Chd4*$^{-/-}$ mice, when the pool of spermatogonia cells is being stablished in the mouse testis. PLZF-positive single, paired, and aligned cells were recognized by their spatial distribution in the seminiferous tubule as previously described. Compared to wild type, we found substantial reduction in the number of single, paired, and aligned spermatogonia in *Chd4*$^{-/-}$ mice (Fig. 4B and C). The reduced number of PLZF-positive cells in *Chd4* mutant testis at 4 dpp indicates that CHD4 regulates the undifferentiated stages of spermatogonia.

To substantiate our finding with whole-mount seminiferous tubule analysis, we stained testes sections from 1-21dpp mice for the expression of PLZF/ZBTB16 (undifferentiated spermatogonia (5, 22)) and TRA98 (all germ cells). Compared to wild type, *Chd4* mutant sections displayed a small reduction in the number of cells expressing TRA98 at both 1dpp and 3dpp (Fig. S6 and S7). We observed equal numbers of SOX9-positive Sertoli cells in testes from wild type and *Chd4*$^{-/-}$ mice at 3, 4, and 9 dpp (Fig. S6B), as expected for the specific loss of *Chd4* in spermatogonia cells. In agreement with that shown in Fig. 4 B and C, both PLZF-positive and TRA98-positive cells were substantially reduced in *Chd4*$^{-/-}$ mutant testis compared to wild type testis at 4 dpp and 7dpp (Fig. S6 and S7).

Given that Chd4 may act as a master regulator of cell-cycle progression, we then examined whether the rapid loss of PLZF-positive spermatogonia in *Chd4*$^{-/-}$ testes was

due to altered proliferative activity. We conducted a BrdU incorporation study to test this possibility. P4 mice were injected with BrdU and analyzed 3 h later, after which we assayed BrdU incorporation in single, paired, and aligned PLZF-positive spermatogonia in whole mounts of seminiferous tubules. We found that all analyzed types of spermatogonia incorporated BrdU in *Chd4*$^{-/-}$ testes at a similar rate as controls (Fig. 4B and C), demonstrating that *Chd4* deficiency does not affect the proliferative activity of PLZF-positive spermatogonia.

CHD4 binds the promoters of genes involved in spermatogonia cell maintenance, and differentiation

To investigate the mechanism of CHD4 requirement in spermatogonia, we aimed to identify genes that are directly regulated by CHD4. We generated genome-wide chromatin-binding profiles of CHD4 in spermatogonia. We prepared enriched fractions of spermatogonia from 5 dpp wild type testes by magnetic-assisted cell separation and analyzed CHD4 chromatin-binding analysis by chromatin immunoprecipitation combined with high-throughput sequencing (ChIP-seq) (Fig. 5, S8A). Heatmaps, aggregate profiles, and direct visualization of profiles revealed a prominent enrichment of CHD4 in promoter regions (Fig. 5A-D and table S1). Hierarchical clustering analysis around ± 3 Kb of gene bodies revealed two major types of CHD4 distribution (Fig. 5A). CHD4 binds to Cluster 1 genes throughout the gene body, with decreasing intensity from the transcription start site (TSS) (Figure 5A and B). In contrast, CHD4 binds to Cluster 2 genes exclusively at the TSS (Fig 5A-C). We identified 2499 CHD4 peaks, distributed mainly in distal intergenic regions (41%), intronic regions (43%) and promoters (25%) (Fig. 5D). These regions often contain regulatory elements, suggesting that CHD4 regulates gene transcription in spermatogonia.

To gain greater insight into the genes potentially regulated by CHD4, we annotated the peaks of CHD4 to the closest gene and performed functional analysis. Analysis of gene ontology (GO) initially revealed 469 genes associated with biological processes, 76 associated with molecular function, and 83 associated with cellular components (p. adjust < 0.05) (table S2-4). The number of genes was reduced to 166, 40, and 30 terms, respectively, after consolidating related/similar terms. We observed approximately 50 genes involved in regulating chromosome organization (including chromosome organization), DNA repair, and the cell cycle (Fig 5E and Fig. S8B). Interestingly, approximately 20 genes were involved in regulating stem cell maintenance and differentiation (Fig 5E and Fig. S8). We noted genes that may be involved in regulating stem cell population maintenance (Floxo3, Hes1, Pax2, Vps72, Eif4e, Tead1, Yap1, and Ctnnnb1) and stem cell differentiation (Hes1, Rest, Tbx5, Sox5, and Setd1A), as their self may regulate transcription (e.g., acting as transcription factors) (Fig. 5F).

CHD4 regulates expression of genes involved in spermatogonia cell survival and differentiation

To investigate the role of CHD4 in regulating gene expression in spermatogonia, we performed genome-wide transcription analysis (RNA-seq) of c-KIT+ (differentiating) and THY1.2+ (undifferentiated) enriched fractions of spermatogonia obtained from wild type and *Chd4* knockout testis. Principal component analysis (PCA) showed substantial differences in the transcriptomes of mutant and wild type c-KIT+ (differentiating) cells, and slight differences in the transcriptomes of THY1.2+ (undifferentiated) mutant and wild type cells (Fig. S9A).

Differential gene expression analysis revealed that loss of CHD4 results in both up- and down-regulated genes in differentiating and undifferentiated spermatogonia (Fig. S10 A-C). We uncovered 3480 up-regulated and 3853 down-regulated genes in

differentiating *Chd4* knockout cells, and 513 up-regulated and 1032 down-regulated genes in undifferentiated *Chd4* knockout (Fig. S10A and B). Down-regulated genes showed the largest magnitude of changes in differentiating cells (Fig. S10C and Fig. S9B). A dispersion estimates plot (Fig. S9C) corroborates that the DESeq2 model used for the analysis of differential gene expression is a good fit of our data.

We noted that genes involved in maintenance and differentiation of stem cells were down-regulated in *Chd4* knockout cells compared to wild type cells, including *Lin28a*, *Piwil2* (23), *Sox3*, *Sohlh2* and *Sall4* in differentiating cells, and *Lmo1*, *Chtf18* and *Sall1* in undifferentiated cells (Fig. S10D). Gene ontology and reactome pathway analysis of the differentially expressed genes showed that CHD4 controls transcription of genes implicated in cell survival (Fig. S10 and Fig. S11). Notably, genes involved in DNA repair (*Ercc4, Nek2, Rad51*), sister chromatid cohesion (*Rad21l* and *Wapl*), and regulation of the cell cycle (*Cdc25*, *Ddc26*, and *Cdc45*) were down-regulated in the absence of CHD4 (Fig. S10E). On the other hand, the genes up-regulated upon loss of CHD4 are related to lipid metabolic pathways, ion homeostasis, processes of the neural system, and involved in muscle contraction; expression of these genes might negatively impact spermatogonia cell fate. Together, our data suggest that CHD4 plays an important role in promoting and repressing the expression of specific genes in wild type spermatogonia.

To uncover genes that are directly regulated by CHD4, we focused on differentially expressed genes with nearby CHD4 binding. We observed 1830 unique genes, with most having a CHD4 signal within the promoter region. In our RNA-seq data set we obtained read counts for 1725 out of the 1830 genes with a CHD4 ChIP-seq peak, covering most of the genes of interest for the analysis (Fig. 6). Principal component analysis (PCA) showed clear differences between wild type and *Chd4* knockout in both c-KIT+ and THY1.2+ affinity purified cells (Fig. S12A), and analysis of dispersion estimates validated subsequent analysis of differential gene expression (Fig. S12B).

We observed 48 up-regulated and 109 down-regulated genes in *Chd4* knockout THY1.2+ cells, as well as 416 up-regulated and 359 down-regulated genes in *Chd4* knockout c-KIT+ cells (Fig. 6A and B). Among the differentially expressed genes, we noted those involved in basic cellular metabolic activities that are required for cell survival (Fig. 6C-E).

Gene ontology and reactome pathway analysis revealed that the subset of potential direct targets that are down-regulated upon loss of CHD4 function in cell survival and proliferation (Fig. S13). Thus, CHD4-mediated regulation of chromatin accessibility or recruitment of transcription factors in wild type cells might be required to directly activate these genes. On the contrary, for those genes that are up-regulated, CHD4 may be directly involved in their repression in the wild type spermatogonia. The terms enriched for undifferentiated cells correspond mainly to down-regulated genes, but we do not exclude that the up-regulated genes might need to be repressed in the wild type condition. The scarcity of enriched terms for up-regulated genes are mainly due to the few significantly differentially expressed genes identified in undifferentiated THY1.2+ cells (157) when the analysis is restricted to genes with a nearby ChIP-Seq signal.

In sum, our results show that CHD4 participates in the establishment and/or maintenance of spermatogonia stem cell through transcriptional regulation of genes participating in critical cell functions impacting cell survival and differentiation.

Discussion

In this work, we examined the potential function of two critical NURD catalytic subunits, CHD4 and CHD3, in spermatogenesis. Our data suggest that a CHD4-NURD (but not CHD3-NURD) complex controls spermatogonia development at early stages of testis development (Fig. 7). Germline deletion of *Chd4,* but not *Chd3,* results in a severe loss of

gametocytes specifically at early stages of the testis cord development. *Chd4* deletion specifically affects spermatogonia, with the first obvious consequences in undifferentiated spermatogonia, and no apparent effect in meiotic process such as repair of double-strand breaks and homologous chromosome interactions. The latter was unexpected because CHD4 is recruited to damaged DNA and promotes homologous recombination-dependent repair of DNA double-strand breaks in somatic cells (24).

Most CHDs are expressed in testis; however, their insertion into the NURD complex seems to be developmentally regulated, with different patterns of expression during gametogenesis. CHD5 (5-7) has been shown to be expressed and required to compact chromatin in the late stages of spermatogenesis (25, 26). In contrast, our results show that CHD4 is expressed and functions at early stages of gametogenesis. We found that the composition of the NURD complex changes as spermatogenesis progresses, with loss of specific subunits in primary spermatocytes. This loss of subunits is consistent with our findings that CHD4-NURD is not required after spermatocytes are committed to meiosis, and suggests that the composition of NURD complexes may define their functions.

The function of CHD4-NURD in spermatogonia development and male gametogenesis is further revealed by our genome-wide analysis of CHD4 chromatin binding, combined with transcriptome analyses of enriched fractions of mouse spermatogonia cells. We show that CHD4 binds and influences the transcription of a number of genes participating in critical cellular processes required for cell maintenance (Fig. 7). This regulation of gene expression possibly operates through local changes in chromatin conformation at genes participating in nucleic acid metabolism (e.g. *Ercc4*, *Nek2*, *Rad21l*, *Tnks2*) and regulation of the cell cycle (e.g. *Cdc45,* Cdc25). Our results

also argue for a possible role of CHD4 in spermatogonia differentiation and cell lineage specification. Indeed, genes involved in cell maintenance and differentiation of stem cells were down regulated in Chd4 knockout cells, indicating that CHD4 promotes their expression in the wild type condition. On the contrary, the genes up regulated upon loss of CHD4 are related to processes that might negatively impact spermatogonia cell fate, such those influencing processes of the neural system and involved in muscle contraction.

Chromatin remodeling complexes are a vast group of regulators with diverse functions in critical cellular processes such as transcription and DNA metabolism. They have been generally classified into four different families SWI/SNF, INO80, ISWI, and NURD (27). Most of the knowledge we have regarding their functions come from studies of somatic cultured cell models. More recently, however, work from different labs has begun exploring the role of chromatin remodelers in germ cell development. Germline-specific deletion of *Brg1* (28) or *Brd7* (29, 30), both components of the SWI/SNF complex, results in gonadal developmental defects. Deletion of *Ino80* in mouse spermatocyte resulted in a similar phenotype to that described for loss of SWI/SNF, with regard to meiotic prophase I failure in recombination and homologous chromosome associations (29). On the contrary, ISWI (31) and CHD5 (32-34), the latter an alternative catalytic subunit of NURD complexes, function late in germ cell development with postmeiotic phenotypes associated with spermiogenesis and fertilization. Collectively, our studies show the unique cellular and molecular requirements of CHD4-NURD in early stages of gamete development. These results support a model in which distinct chromatin remodeling complexes fulfill specific requirements during different stages of gamete development.

Material and Methods

Mice

CHD4-floxed mice (*CHD4*$^{fl/fl}$) have been described (Williams et al 2004). *Chd3*-floxed mice were generated by Cyagen Biosciences using homologous recombination of a targeting vector in C57Bl/6 embryonic stem cells. The targeting vector incorporated a 5' LoxP site inserted between exons 12 and 13 and a 3' LoxP site inserted between exons 20 and 21 of the wild type *Chd3* allele. Transgenic *Cre* recombinase mice *Ddx4-Cre*$^{FVB\text{-}Tg(Ddx4\text{-}cre)1Dcas/J}$ or *Stra8-iCre*$^{B6.FVB\text{-}Tg(Stra8\text{-}icre)1Reb/LguJ}$ were purchased from The Jackson Laboratory (Bar Harbor, ME). *Spo11*-Cre mice were provided by Dr. P. Jordan (Johns Hopkins University Bloomberg School of Public Health, Baltimore, MD). *Chd3 or Chd4* gonad-specific knockouts and wild-type heterozygotes littermates were obtained from crosses between female homozygous *flox/flox* mice with male heterozygous Cre/+; *Chd3* Wt/flox and/or *Chd4* Wt/flox mice.

All experiments conformed to relevant regulatory standards guidelines and were approved by the Oklahoma Medical Research Foundation-IACUC (Institutional Animal Care and Use Committee).

Mice Genotyping

Characterization of wild type and *floxed* alleles was carried out by PCR using the following oligonucletides: CHD3 forward 5'-GGGTGGAGGTGGAAAGTGTA, CHD3 reverse 5'-AGAGGACAGGTCACAGGACAA, CHD4 forward 5'- TCCAGAAGAAGACGGCAGAT and CHD4 reverse 5'- CTGGTCATAGGGCAGGTCTC. The presence of *cre* recombinase allele were determine by PCR using the following primers: SPO11-Cre forward 5'-CCATCTGCCACCAGCCAG, SPO11-Cre reverse 5'-TCGCCATCTTCCAGCAGG, DDX4-Cre forward 5'-CACGTGCAGCCGTTTAAGCCGCGT, DDX4-Cre reverse 5'-TTCCCATTCTAAACAACACCCTGAA, STRA8-iCre forward 5'-

AGATGCCAGGACATCAGGAACCTG and STRA8-iCre reverse 5'-ATCAGCCACACCAGACAGAGAGATC.

Real time-PCR

Total RNA was isolated from adult testis or from enriched fractions of spermatogonia with the Direct-zol RNA MiniPrep Plus kit (Zymo Research). RNA (2.0µg) was oligo-dT primed and reverse-transcribed with the High capacity RNA-to-cDNA kit (Applied Biosystems). Exon boundaries of *Chd4 and Chd3* were amplified using TaqMan Assays (Applied Biosystems) as directed by the manufacturer using Beta-2 macroglobulin as standard. TaqMan Mm01190896_m1 (*Chd4*), Mm01332658_m1 (CHD3), and Mm00437762_m1 (Beta-2 microglobulin). Gene expression was normalized with respect to wild type with wild type expression levels considered to be 1.

Histology and immunostaining

Preparation, immunostaining, and analysis of whole mount seminiferous tubules was performed as previously described(35). Testes and ovaries were dissected, fixed in 10% neutral-buffered formalin (Sigma) and processed for paraffin embedding. After sectioning (5–8-μm), tissues were positioned on microscope slides and analyzed using hematoxylin and eosin using standard protocols. For immunostaining analysis, tissue sections were deparaffinized, rehydrated and antigen was recovered in sodium citrate buffer (10 mM Sodium citrate, 0.05% Tween 20, pH 6.0) by heat/pressure-induced epitope retrieval. Incubations with primary antibodies were carried out for 12 h at 4°C in PBS/BSA 3%. Primary antibodies used in this study were as follows: monoclonal mouse antibody raised against mouse SOX9 at 1 : 500 dilution (EMD Millipore – AB5535), polyclonal rabbit antibody raised against mouse STRA8 at 1 : 500 dilution (AbCam, ab49602), polyclonal

rabbit antibody raised against mouse TRA98 at 1 : 200 dilution (AbCam, 82527), monoclonal mouse antibody raised against mouse PLZF at 1 : 50 dilution (Santa Cruz, 28319), polyclonal chicken antibody raised against mouse SYCP3 at 1 : 300 dilution (our laboratory), polyclonal rabbit antibody raised against mouse SYCP1 at 1 : 100 dilution (Novus, NB300-229), monoclonal mouse antibody raised against γH2AX (Ser139) at 1 : 1000 dilution (Millipore, 05-636). Following three washes in 1 X PBS, slides were incubated for 1 h at room temperature with secondary antibodies. A combination of Fluorescein isothiocyanate (FITC)-conjugated goat anti-rabbit IgG (Jackson laboratories) with Rhodamine-conjugated goat anti-mouse IgG and Cy5-conjugated goat anti-human IgG each diluted 1:450 were used for simultaneous triple immunolabeling. Slides were subsequently counterstained for 3 min with 2µg/ml DAPI containing Vectashield mounting solution (Vector Laboratories) and sealed with nail varnish. We use Axiovision SE 64 (Carl Zeiss, inc.) for imaging acquisition and processing.

Purification of Spermatogonia

Testis from 7dpp mice were incubated in Dulbecco's Modified Eagle Medium (DMEM) containing 1 mg/mL of collagenase, 300 U/mL of hyaluronidase and 5 mg/mL DNAse I (StemCell Technologies). Seminiferous tubules were then incubated of with 0.05% Trypsin-EDTA solution (Mediatech Inc). Trypsin digestion was stopped with 1% BSA and single cell suspension was obtained by mechanical resuspension followed by filtration through a 40-µm-pore-size cell strainer. Differentiating spermatogonias (c-KIT+) were magnetically labeled with CD117 (c-KIT+) MicroBeads (MACS Miltenyi Biotec) and isolated using MS columns according to manufacturer's instructions. After the depletion of the c-KIT+ spermatogonias, the population of undifferentiated spermatogonias were separated using CD90.2 (THY1.2+) MicroBeads.

Primary spermatocyte enrichment

Synchronized mice pachytene spermatocytes obtained from the first spermatogenic wave were purified as described in (25, 26).

Statistical Analyses

Results are presented as mean ± standard deviation (SD). Statistical analysis was performed using Prism Graph statistical software. Two-tailed unpaired Student's *t*-test was used for comparisons between 2 groups. $P < 0.05$ was considered statistically significant.

ChIP-seq

Undifferentiated and differentiating spermatogonia cell fractions were obtained by affinity purification (C-KIT and THY1, respectively) of total wild type testis. ChIP was performed as previously described with modifications (32). Cells were fixed for 5 min 1% methanol-free formaldehyde, quenched for 5 min with 125 mM glycine, washed twice with PBS1X and ressuspended in 5 mL of PBS1X containing 1mM of PMSF. Cells were dounced 20 strokes with a 'B' pestle, and then, pelleted at 2000 rpm for 5 min at 4°C. The cells were ressuspended in in 5 mL of Lysis buffer 1 containing 1mM PMSF (10 mM Tris-HCl pH8, 10 mM EDTA, 0.5 mM EGTA, 0.25% Triton X-100) and centrifuged at 2000 rpm for 5 min at 4°C. The same procedure was repeated with 5mL of Lysis buffer 2 containing 1mM PMSF (10 mM Tris-HCl pH8, 1 mM EDTA, 0.5 mM EGTA, 200 mM NaCl). The cells were finally resuspended in 1 mL of ChIP buffer containing 1X protease inhibitor cocktail, Roche (50 mM Tris-HCl pH8, 1 mM EDTA, 150 mM NaCl, 1% Triton X-100, 0.1% Na deoxycholate, 0.1% SDS) and sonicated for 15 minutes using the Covaris E220 evolution. The sample was cleared at 12,000 g for 10 min at 4°C, and the chromatin was incubated

with anti-CHD4 antibody (ab 70469, Abcam) overnight at 4°C. Antibody/chromatin complexes were captured with ChIP-grade protein A/G magnetic beads (ThermoFisher) for 2 h at 4°C and washed 2 times with increasing salt concentration (20 mM Tris-HCl pH8, 2 mM EDTA, 150-500 mM NaCl , 1% Triton X-100, 0.1% Na deoxycholate) and once with a Litium buffer (10 mM Tris-HCl pH8, 1 mM EDTA, 250 mM LiCl , 1% Igepal, 0.7% Na deoxycholate). The beads were washed twice with TE buffer pH7.4 (10 mM Tris-HCl, 1 mM EDTA) and DNA was eluted at 65°C with agitation for 30 minutes using 150 uL 1% SDS + 100 mM NaHCO3 made freshly (twice). Cross-links were reversed overnight by adding 5 uL of 5 M NaCl and incubating at 65°C. DNA was treated with 3 uL RNaseA for 30 min at 37° C and then proteinase K for 1 h at 56° C. The DNA is purified using the miniElute PCR purification kit (Qiagen) and quantified using Qubit (Life Technologies) before library preparation (in-house or Kapa Hyperprep kit (KR0961)). Sequencing was performed on Illumina NextSeq 500 instrument in the OMRF Genomics core.

ChIP-seq data analysis

Quality metrics of the sequenced reads were computed using the tools FastQC (version 0.11.8), FastQ Screen (version 0.13.0) and AdapterRemoval (version 2.1.7)(36). Pair end 75 bp reads from two independent experiments were aligned to mm10 using bwa (Version 0.7.17)(37, 38). Picard (version 2.17.8) and SAMtools (version 1.9) were used to obtain mapping quality metrics, remove duplicates and filter unique reads (39, 40). Only the uniquely aligned reads passing the quality filtering were selected for calculations reported here. MultiQC (version 1.7) was used to generate metrics reports (41). The predominant insert-size (fragment length) based on strand cross-correlation peak was computed using phantompeaksqualtools (version 1.14)(42). Bigwig coverage tracks were generated using bamCoverage tool from deepTools (version 3.1.3)(43, 44), with a binsize of 50 bp and extending fragments to 300bp and further smooth length 150 bp. Average profiles and

heatmaps were plot using Deeptools (Peaks were called using MACS (version 2.1.2)(45, 46) using the broad mode and the following parameters: broad-cutoff 0.05, nomodel, extsize 200. In addition, we filter the peaks against the ENCODE blacklist regions and we further merged any peaks within 500 bp of the nearest peakusing bedtools (version 2.27.1)(47). Peaks annotation and functional analysis was implemented in the R statistical software (www.R-project.org). Peaks were annotated for the nearest transcription start site using ChIPseeker package(48) and the annotation was based on org.Mm.eg.db mapping using Entrez Gene identifiers. Gene ontology analysis was done using clusterProfiler package(49). The simplify function from clusterProfiler package with a cutoff of 0.7 was applied to remove redundant terms.

RNA-seq data analysis

Quality metrics of the sequenced reads were computed as described above (see ChIP-seq analysis). Pair end 75 bp reads from four independent experiments were aligned to mm10 using STAR (Version 2.7)(50, 51). Uniquely aligned reads passing the quality filtering were processed into gene level counts using featureCounts (version1.6.2) and Genecode V20 annotations(52). Differential expression was carried out using DESeq2 (version 1.22.2)(53) using an FDR of 0.05, fold change cutoff = 1.5, and mean of normalized counts cutoff of 50. Differential expressed genes were clustered and visualized using the pheatmap function in R. Gene ontology and Reactome pathway analysis was done using clusterProfiler and ReactomePA package(54). The simplify function from clusterProfiler package with a cutoff of 0.7 was applied to remove redundant terms.

Acknowledgments. We thank Angela Andersen from Life Science Editors editorial services for her assistance in manuscript writing.

References

1. L. Wang, Z. Xu, M. B. Khawar, C. Liu, W. Li, The histone codes for meiosis. *Reproduction* **154**, R65-R79 (2017).
2. F. K. Stanley, S. Moore, A. A. Goodarzi, CHD chromatin remodelling enzymes and the DNA damage response. *Mutat. Res.* **750**, 31-44 (2013).
3. A. A. Goodarzi, T. Kurka, P. A. Jeggo, KAP-1 phosphorylation regulates CHD3 nucleosome remodeling during the DNA double-strand break response. *Nat. Struct. Mol. Biol.* **18**, 831-839 (2011).
4. D. H. Larsen *et al.*, The chromatin-remodeling factor CHD4 coordinates signaling and repair after DNA damage. *J. Cell Biol.* **190**, 731-740 (2010).
5. M. R. Pan *et al.*, Chromodomain helicase DNA-binding protein 4 (CHD4) regulates homologous recombination DNA repair, and its deficiency sensitizes cells to poly(ADP-ribose) polymerase (PARP) inhibitor treatment. *J. Biol. Chem.* **287**, 6764-6772 (2012).
6. S. E. Polo, A. Kaidi, L. Baskcomb, Y. Galanty, S. P. Jackson, Regulation of DNA-damage responses and cell-cycle progression by the chromatin remodelling factor CHD4. *EMBO J.* **29**, 3130-3139 (2010).
7. C. R. Clapier, B. R. Cairns, The biology of chromatin remodeling complexes. *Annu. Rev. Biochem.* **78**, 273-304 (2009).
8. M. P. Torchy, A. Hamiche, B. P. Klaholz, Structure and function insights into the NuRD chromatin remodeling complex. *Cell. Mol. Life Sci.* **72**, 2491-2507 (2015).
9. J. A. Eisen, K. S. Sweder, P. C. Hanawalt, Evolution of the SNF2 family of proteins: subfamilies with distinct sequences and functions. *Nucleic Acids Res.* **23**, 2715-2723 (1995).
10. A. Sada, A. Suzuki, H. Suzuki, Y. Saga, The RNA-binding protein NANOS2 is required to maintain murine spermatogonial stem cells. *Science* **325**, 1394-1398 (2009).
11. K. Gassei, K. E. Orwig, SALL4 expression in gonocytes and spermatogonial clones of postnatal mouse testes. *PLoS One* **8**, e53976 (2013).
12. K. Bouazoune *et al.*, The dMi-2 chromodomains are DNA binding modules important for ATP-dependent nucleosome mobilization. *EMBO J.* **21**, 2430-2440 (2002).
13. R. Morra, B. M. Lee, H. Shaw, R. Tuma, E. J. Mancini, Concerted action of the PHD, chromo and motor domains regulates the human chromatin remodelling ATPase CHD4. *FEBS Lett.* **586**, 2513-2521 (2012).
14. R. E. Mansfield *et al.*, Plant homeodomain (PHD) fingers of CHD4 are histone H3-binding modules with preference for unmodified H3K4 and methylated H3K9. *J. Biol. Chem.* **286**, 11779-11791 (2011).
15. A. A. Watson *et al.*, The PHD and chromo domains regulate the ATPase activity of the human chromatin remodeler CHD4. *J. Mol. Biol.* **422**, 3-17 (2012).
16. C. A. Musselman *et al.*, Binding of the CHD4 PHD2 finger to histone H3 is modulated by covalent modifications. *Biochem. J.* **423**, 179-187 (2009).
17. G. Margolin, P. P. Khil, J. Kim, M. A. Bellani, R. D. Camerini-Otero, Integrated transcriptome analysis of mouse spermatogenesis. *BMC Genomics* **15**, 39 (2014).
18. H. Hoffmeister *et al.*, CHD3 and CHD4 form distinct NuRD complexes with different yet overlapping functionality. *Nucleic Acids Res.* **45**, 10534-10554 (2017).
19. H. F. Allen, P. A. Wade, T. G. Kutateladze, The NuRD architecture. *Cell. Mol. Life Sci.* **70**, 3513-3524 (2013).

20. T. Gallardo, L. Shirley, G. B. John, D. H. Castrillon, Generation of a germ cell-specific mouse transgenic Cre line, Vasa-Cre. *Genesis* **45**, 413-417 (2007).
21. M. Pellegrini *et al.*, Targeted JAM-C deletion in germ cells by Spo11-controlled Cre recombinase. *J. Cell Sci.* **124**, 91-99 (2011).
22. W. Qi *et al.*, Acetyltransferase p300 collaborates with chromodomain helicase DNA-binding protein 4 (CHD4) to facilitate DNA double-strand break repair. *Mutagenesis* **31**, 193-203 (2016).
23. Q. E. Yang, J. M. Oatley, Spermatogonial stem cell functions in physiological and pathological conditions. *Curr. Top. Dev. Biol.* **107**, 235-267 (2014).
24. T. Sasaki, A. Shiohama, S. Minoshima, N. Shimizu, Identification of eight members of the Argonaute family in the human genome. *Genomics* **82**, 323-330 (2003).
25. W. Li *et al.*, Chd5 orchestrates chromatin remodelling during sperm development. *Nat Commun* **5**, 3812 (2014).
26. T. Zhuang *et al.*, CHD5 is required for spermiogenesis and chromatin condensation. *Mech. Dev.* **131**, 35-46 (2014).
27. J. Fujikura *et al.*, Differentiation of embryonic stem cells is induced by GATA factors. *Genes Dev.* **16**, 784-789 (2002).
28. J. Yodh, ATP-Dependent Chromatin Remodeling. *Adv. Exp. Med. Biol.* **767**, 263-295 (2013).
29. Y. Kim, A. M. Fedoriw, T. Magnuson, An essential role for a mammalian SWI/SNF chromatin-remodeling complex during male meiosis. *Development* **139**, 1133-1140 (2012).
30. J. Wang, H. Gu, H. Lin, T. Chi, Essential roles of the chromatin remodeling factor BRG1 in spermatogenesis in mice. *Biol. Reprod.* **86**, 186 (2012).
31. D. W. Serber, J. S. Runge, D. U. Menon, T. Magnuson, The Mouse INO80 Chromatin-Remodeling Complex Is an Essential Meiotic Factor for Spermatogenesis. *Biol. Reprod.* **94**, 8 (2016).
32. J. A. Dowdle *et al.*, Mouse BAZ1A (ACF1) is dispensable for double-strand break repair but is essential for averting improper gene expression during spermatogenesis. *PLoS Genet* **9**, e1003945 (2013).
33. T. J. Broering *et al.*, BAZ1B is dispensable for H2AX phosphorylation on Tyrosine 142 during spermatogenesis. *Biol Open* **4**, 873-884 (2015).
34. P. J. Thompson, K. A. Norton, F. H. Niri, C. E. Dawe, H. E. McDermid, CECR2 is involved in spermatogenesis and forms a complex with SNF2H in the testis. *J. Mol. Biol.* **415**, 793-806 (2012).
35. K. Gassei, H. Valli, K. E. Orwig, Whole-mount immunohistochemistry to study spermatogonial stem cells and spermatogenic lineage development in mice, monkeys, and humans. *Methods Mol. Biol.* **1210**, 193-202 (2014).
36. K. A. Romer, D. G. de Rooij, M. L. Kojima, D. C. Page, Isolating mitotic and meiotic germ cells from male mice by developmental synchronization, staging, and sorting. *Dev. Biol.* **443**, 19-34 (2018).
37. M. Schubert, S. Lindgreen, L. Orlando, AdapterRemoval v2: rapid adapter trimming, identification, and read merging. *BMC Res. Notes* **9**, 88 (2016).
38. S. Lindgreen, AdapterRemoval: easy cleaning of next-generation sequencing reads. *BMC Res. Notes* **5**, 337 (2012).
39. H. Li, R. Durbin, Fast and accurate short read alignment with Burrows-Wheeler transform. *Bioinformatics* **25**, 1754-1760 (2009).
40. H. Li, R. Durbin, Fast and accurate long-read alignment with Burrows-Wheeler transform. *Bioinformatics* **26**, 589-595 (2010).
41. H. Li *et al.*, The Sequence Alignment/Map format and SAMtools. *Bioinformatics* **25**, 2078-2079 (2009).

42. P. Ewels, M. Magnusson, S. Lundin, M. Kaller, MultiQC: summarize analysis results for multiple tools and samples in a single report. *Bioinformatics* **32**, 3047-3048 (2016).
43. S. G. Landt *et al.*, ChIP-seq guidelines and practices of the ENCODE and modENCODE consortia. *Genome Res.* **22**, 1813-1831 (2012).
44. P. V. Kharchenko, M. Y. Tolstorukov, P. J. Park, Design and analysis of ChIP-seq experiments for DNA-binding proteins. *Nat. Biotechnol.* **26**, 1351-1359 (2008).
45. J. T. Robinson *et al.*, Integrative genomics viewer. *Nat. Biotechnol.* **29**, 24-26 (2011).
46. H. Thorvaldsdottir, J. T. Robinson, J. P. Mesirov, Integrative Genomics Viewer (IGV): high-performance genomics data visualization and exploration. *Brief Bioinform* **14**, 178-192 (2013).
47. Y. Zhang *et al.*, Model-based analysis of ChIP-Seq (MACS). *Genome Biol.* **9**, R137 (2008).
48. A. R. Quinlan, I. M. Hall, BEDTools: a flexible suite of utilities for comparing genomic features. *Bioinformatics* **26**, 841-842 (2010).
49. G. Yu, L. G. Wang, Q. Y. He, ChIPseeker: an R/Bioconductor package for ChIP peak annotation, comparison and visualization. *Bioinformatics* **31**, 2382-2383 (2015).
50. M. Ashburner *et al.*, Gene ontology: tool for the unification of biology. The Gene Ontology Consortium. *Nat. Genet.* **25**, 25-29 (2000).
51. G. Yu, L. G. Wang, Y. Han, Q. Y. He, clusterProfiler: an R package for comparing biological themes among gene clusters. *OMICS* **16**, 284-287 (2012).
52. A. Dobin *et al.*, STAR: ultrafast universal RNA-seq aligner. *Bioinformatics* **29**, 15-21 (2013).
53. Y. Liao, G. K. Smyth, W. Shi, featureCounts: an efficient general purpose program for assigning sequence reads to genomic features. *Bioinformatics* **30**, 923-930 (2014).
54. M. I. Love, W. Huber, S. Anders, Moderated estimation of fold change and dispersion for RNA-seq data with DESeq2. *Genome Biol.* **15**, 550 (2014).

Figure Legends

Figure 1. CHD4 expression and formation of different NURD complexes during gametogenesis. (A) Expression of *Chd4* monitored by immunofluorescence in testis sections of 14dpp and 2 months (adult) old mouse using two distinct antibodies against CHD4, a rabbit polyclonal anti-CHD4 and anti-PLZF (top panel) and mouse monoclonal anti-CHD4 and anti-SOX9 (bottom panel). Arrows indicate examples of CHD4 positive spermatogonia (PLZF) and Sertoli (SOX9) cells. **(B)** Testis sections of 2 months old mouse immunostained with antibodies specific for CHD4, SYCP3 and γH2AX (the last two

markers of primary spermatocytes) (a and b). Blue arrows indicate examples of spermatogonia and white arrowheads indicate Sertoli cells. Quantification of relative fluorescence intensity in spermatogonia (Sper), Sertoli (Sert.), preleptotene/leptotene/zygotene (P-Z), and pachytene (Pach.) cells is also shown. **(C)** Western blot analysis of different NURD components in Sertoli cells (SOX9 positive), undifferentiated (THY1.2+) and differentiating spermatogonia (c-KIT+) (STRA8 positive), and pachytene primary spermatocytes (SYCP3 positive). Lamin B (Lam B) and α-tubulin (Tub) was used as loading standards. The scheme represents the composition of a canonical NURD complex. **(D)** CHD4-participating NURD complexes in spermatogonia and Sertoli cells assessed by coimmunoprecipitation with anti-CHD4 as a bate. Non-specific IgG was used as a bait control. The star marks an unspecific reactive band.

Figure 2. *Chd4* and *Chd3* gene targeting design and testis developmental defects in *Chd4* mutant mice. (A and B) Testis specific Cre knockout strategy for deletion of *Chd4* and *Chd3*. See description in the text. **(C)** The panel shows expected time of expression for Ddx4-Cre and Spo11-Cre used in this study. **(D)** *Chd4* and *Chd3* transcription levels expression in whole testis **(E)** H&E stained paraffin testis sections of wild type, Ddx4-*Chd4*$^{-/-}$, Spo11-*Chd4*$^{-/-}$, and Ddx4-*Chd3*$^{-/-}$ mice. Quantification of testis weight for wild type and homozygous knockout mice is also shown.

Figure 3. Ddx4-*Chd4*$^{-/-}$ mice show profound defects in gametogenesis. (A) H&E stained histological sections of wild type and Ddx4-*Chd4*$^{-/-}$ testis. Stars mark seminiferous tubules with absent germ cells. Note unchanged number and morphology of Sertoli cells (indicated by green arrows). **(B)** Histological sections of wild type and Ddx4-*Chd4*$^{-/-}$ testis showing seminiferous tubules immunolabeled with SOX9 (a marker of Sertoli cells) and

TRA98 (to mark germ cells). P, pachytene cells; Se, Sertoli cells; Rs, rounded spermatids. **(C)** H&E stained histological sections of wild type and Ddx4-*Chd4*$^{-/-}$ ovaries. F, follicles and CL, corpora lutea.

Figure 4. Spermatogonia cell survival and differentiation requires CHD4. (A) Histological sections of wild type and Ddx4-*Chd4*$^{-/-}$ testis cord from 9 days old mice stained with H&E (a and b), immunostained with TRA98 antibodies (marking germ cells, c and d), and Hematoxylin and immunostained with STRA8 antibodies (marking differentiating spermatogonia) (e and f). Arrows mark type of cells present in wild type but reduced in number or absent in the mutant. **(B)** Immunostaining of whole mount seminiferous tubules reveals loss of single, paired and aligned (assessed by spatial distribution) undifferentiated spermatogonia (PLZF) in 4dpp *Chd4*$^{-/-}$ mice. EDU was used to mark proliferating cells. **(C)** Quantitation of number of cell positive for PLZF shown in B. Wild type versus *Chd4*$^{-/-}$ mutants (number of cells corrected by total length of seminiferous tubule analyzed) single (S), paired (P), aligned 3 (Al3), and aligned 4 (Al4) cells. A total of 7.36 mm and 10.15 mm seminiferous tubule length was counted in wild type and *Chd4*$^{-/-}$ mice, respectively. Quantitation of number of EDU positive single, paired, aligned 3, and aligned 4 spermatogonia is also shown.

Figure 5. CHD4 genome-wide chromatin binding profile and analysis. (A) Heatmaps showing CHD4 occupancy centered in transcription start site (TSS) for all genes and in between TSS (left panel) and TES clustered according to the distribution of the signal (right panel). **(B)** Aggregate profiles corresponding to CHD4 signal between TSS and TES according to the distribution of the ChIP-seq signal. **(C)** Examples of CHD4 occupancy at or near a gene promoter assessed by ChIP-seq. **(D)** Venn diagram depicting genomic features associated with CHD4 peaks. **(E)** Gene ontology analysis of genes associated to

CHD4 ChIP-Seq signals**. (F)** Selected genes with associated CHD4 binding sites corresponding to gene ontology and gene functional analysis.

Figure 6. Analysis of genes with CHD4 occupancy and showing transcription changes associated to *Chd4* deletion. (A and **B)** Heatmaps associated to gene expression differences (up- and downregulated) between wild type and *CHD4* knockout undifferentiated (THY1.2+) and differentiating (c-KIT+) spermatogonia. **(C** and **D)** Volcano plots showing differentially expressed genes for a gene subset exhibiting CHD4 occupancy assessed by ChIP-seq in differentiating **(C)** and undifferentiated **(D)** spermatogonia fractions. Gene symbols are shown for some of the genes with most significant changes. **(E)** Gene ontology analysis and associated genes corresponding to biological processes for differentiating and undifferentiated spermatogonia.

Figure 7. Diagram summarizing the proposed functions of CHD4 during early gametogenesis and the effect of *Chd4* deletion in testis development. Undiff Spg: undifferentiated spermatogonia, Diff Spg: differentiating spermatogonia, PI Spc: Pre-leptotene spermatocyte, Primary Spc: primary spermatocytes (leptotene-diplotene), Sec Spc: secondary spermatocyte.

Figure 1

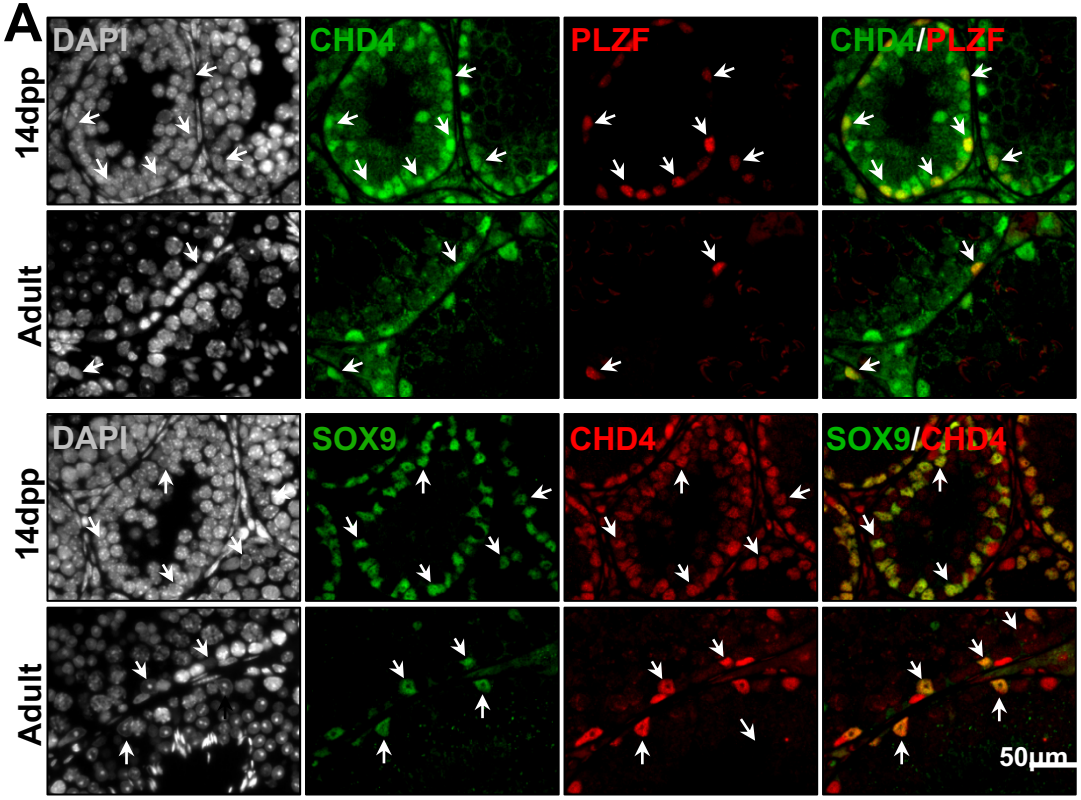
A
DAPI
CHD4
PLZF
CHD4/PLZF
14dpp
Adult
DAPI
SOX9
CHD4
SOX9/CHD4
14dpp
Adult
50μm

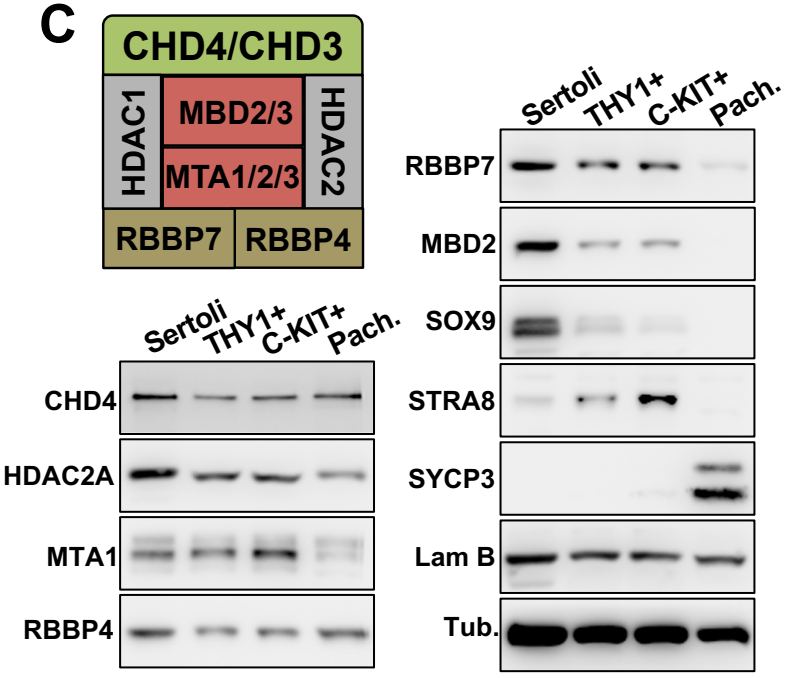
C
CHD4/CHD3
HDAC1
MBD2/3
HDAC2
MTA1/2/3
RBBP7
RBBP4
Sertoli
THY1+
C-KIT+
Pach.
CHD4
HDAC2A
MTA1
RBBP4
RBBP7
MBD2
SOX9
STRA8
SYCP3
Lam B
Tub.

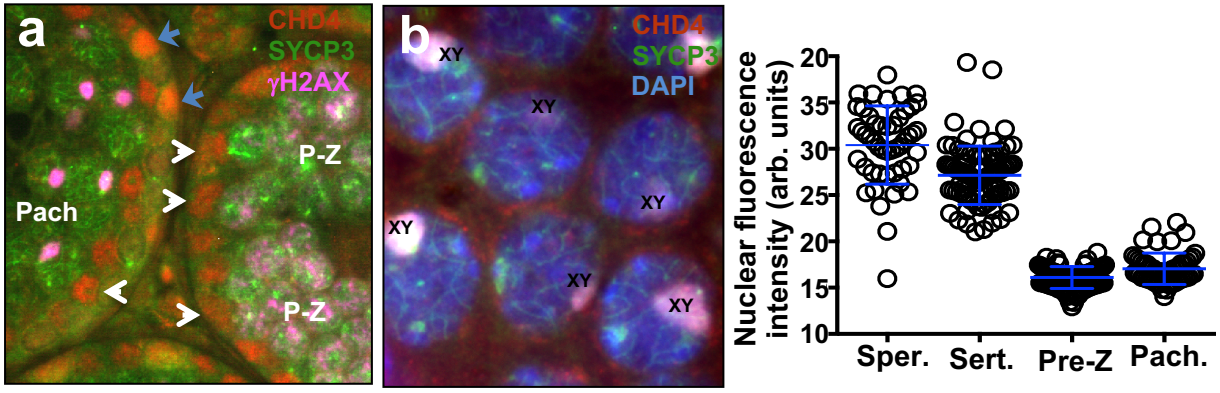
B
a
CHD4
SYCP3
γH2AX
P-Z
Pach
P-Z
b
CHD4
SYCP3
DAPI
XY
Nuclear fluorescence intensity (arb. units)
Sper.
Sert.
Pre-Z
Pach.

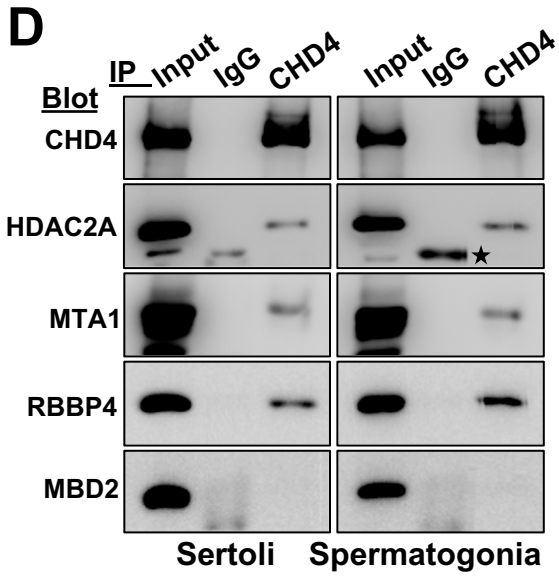
D
IP
Input
IgG
CHD4
Blot
CHD4
HDAC2A
MTA1
RBBP4
MBD2
Sertoli
Spermatogonia

Figure 2

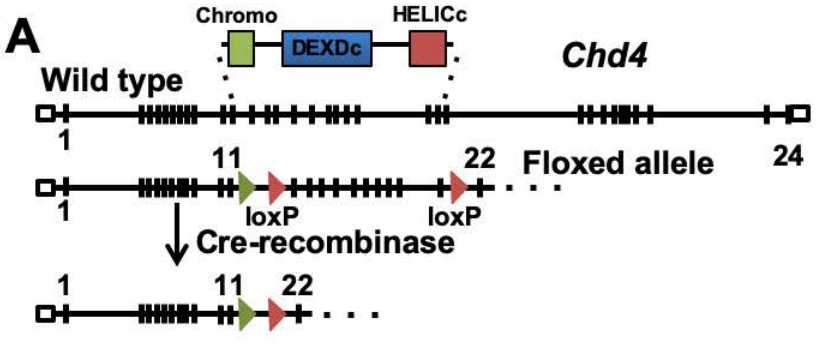
A
Chromo
HELICc
DEXDc
Chd4
Wild type
1
11
22
24
Floxed allele
loxP
loxP
Cre-recombinase

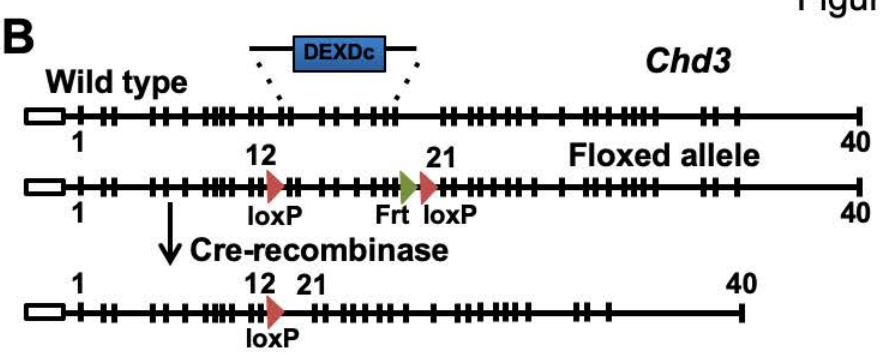
B
DEXDc
Chd3
Wild type
1
12
21
40
Floxed allele
loxP
Frt
loxP
Cre-recombinase


C
Primordial germ cells
Genocytes
Mitosis
Spermatogonia
Meiosis
Spermatocytes
Ddx4-Cre
Spo11-Cre

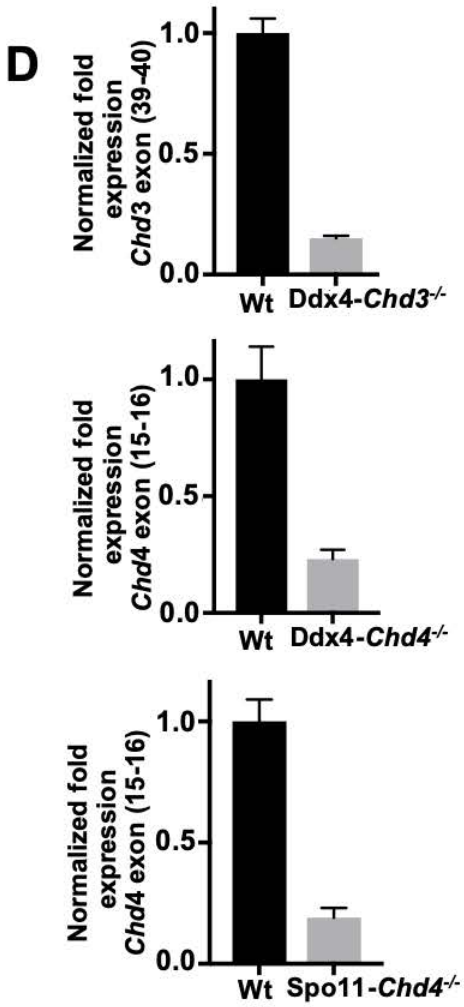
D
Normalized fold expression Chd3 exon (39-40)
Wt
Ddx4-Chd3-/-
Normalized fold expression Chd4 exon (15-16)
Wt
Ddx4-Chd4-/-
Normalized fold expression Chd4 exon (15-16)
Wt
Spo11-Chd4-/-

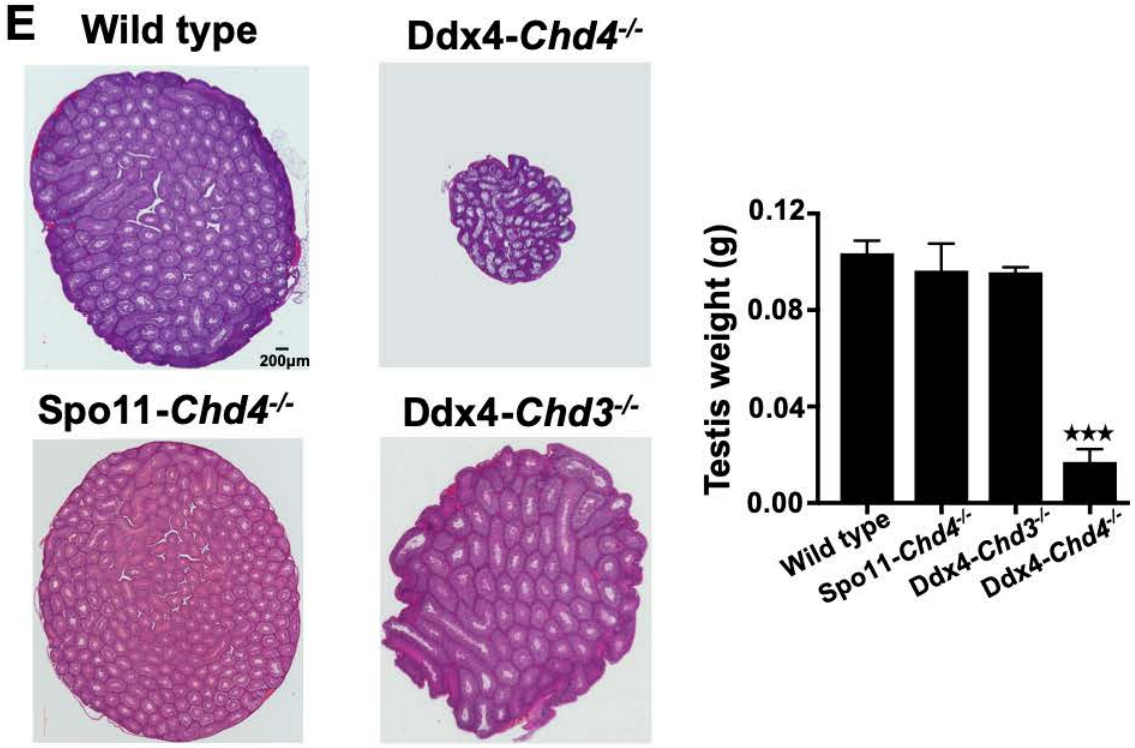
E
Wild type
Ddx4-Chd4-/-
200µm
Spo11-Chd4-/-
Ddx4-Chd3-/-
Testis weight (g)
Wild type
Spo11-Chd4-/-
Ddx4-Chd3-/-
Ddx4-Chd4-/-

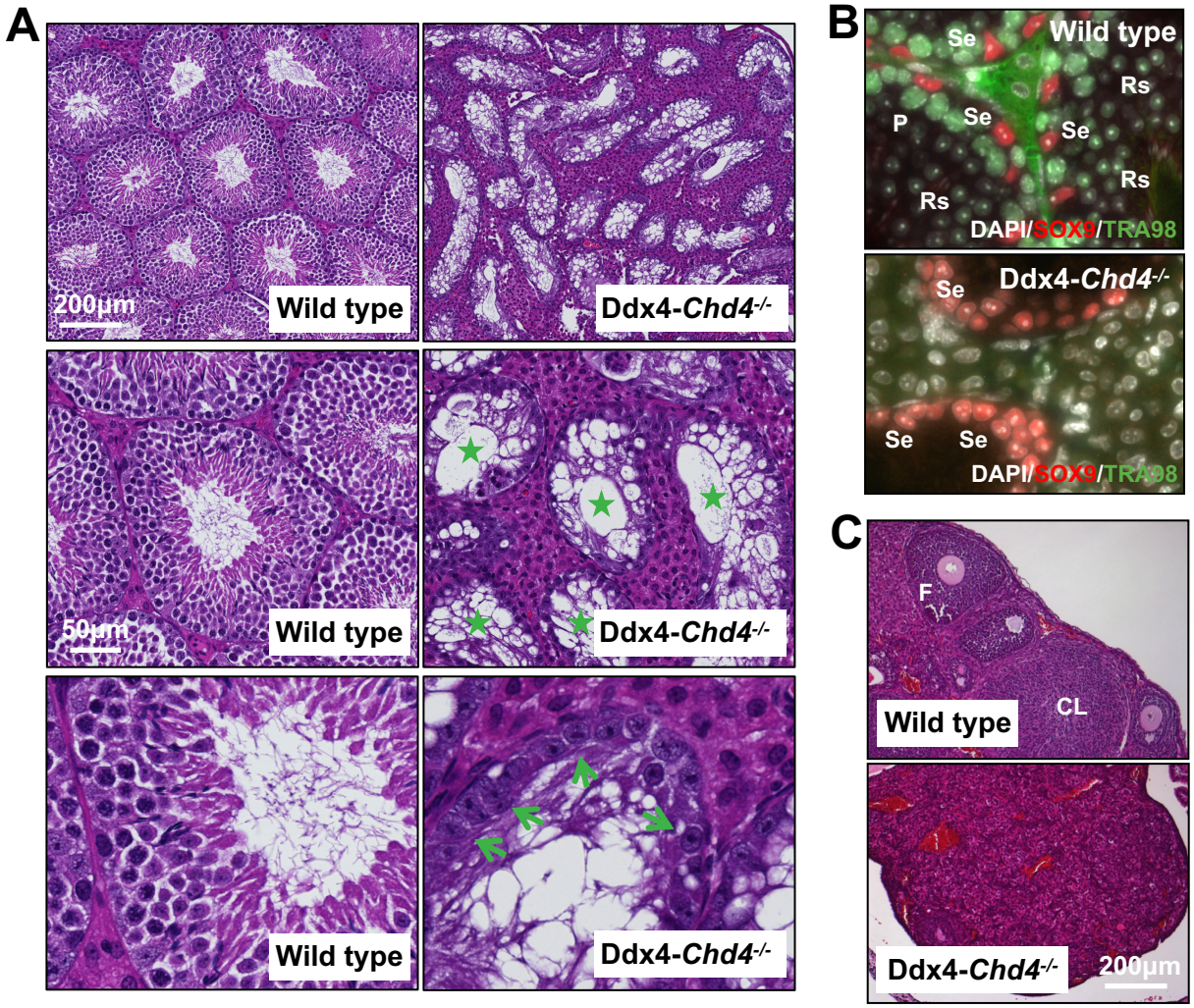
A
200μm
Wild type
Ddx4-Chd4-/-
50μm
Wild type
Ddx4-Chd4-/-
Wild type
Ddx4-Chd4-/-
B
Se
Wild type
Rs
P
Se
Se
Rs
Rs
DAPI/SOX9/TRA98
Se
Ddx4-Chd4-/-
Se
Se
Se
DAPI/SOX9/TRA98
C
F
CL
Wild type
Ddx4-Chd4-/-
200μm

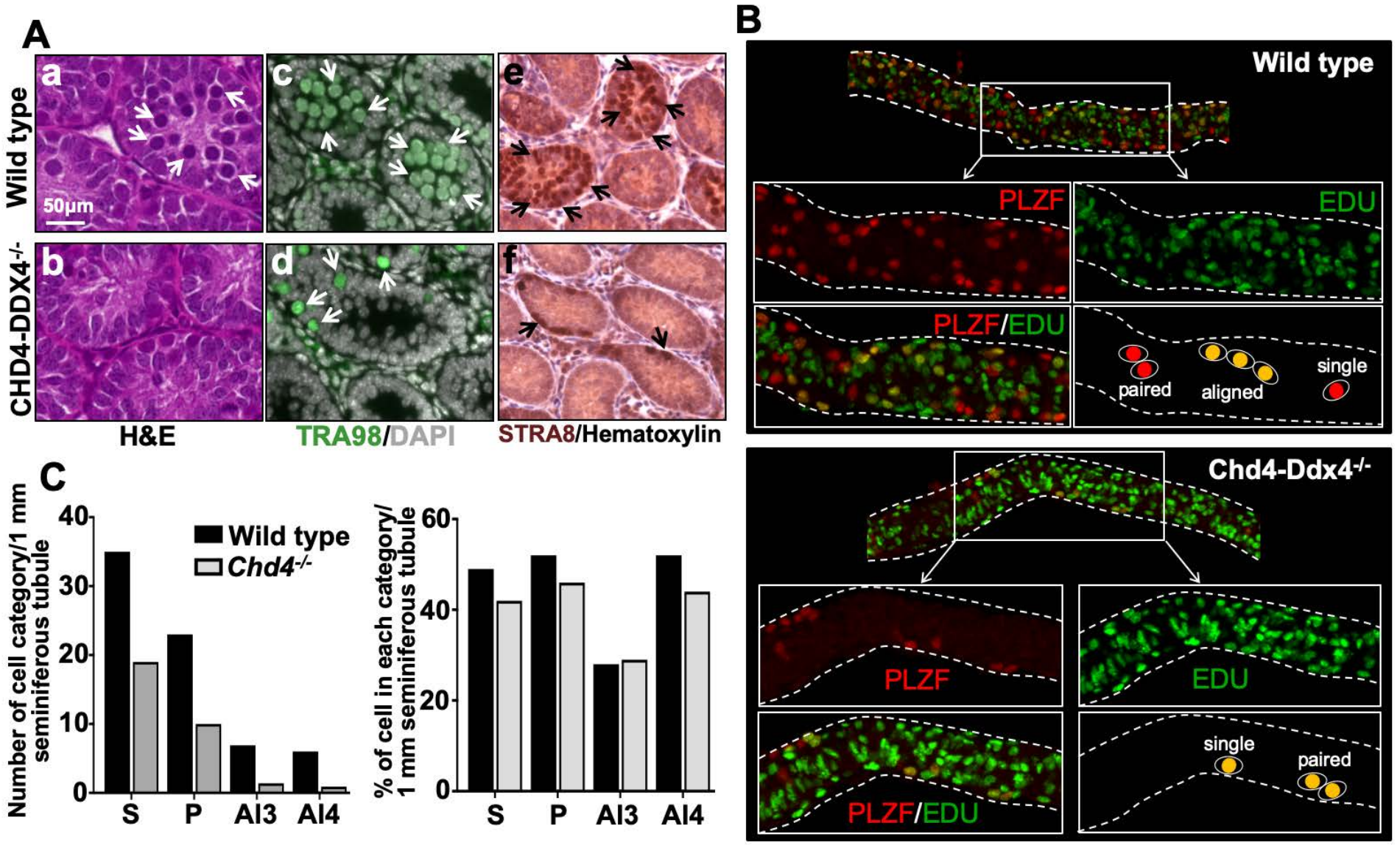
A
Wild type
CHD4-DDX4-/-
a
b
c
d
e
f
50μm
H&E
TRA98/DAPI
STRA8/Hematoxylin
B
Wild type
PLZF
EDU
PLZF/EDU
paired
aligned
single
Chd4-Ddx4-/-
PLZF
EDU
PLZF/EDU
single
paired
C
Number of cell category/1 mm seminiferous tubule
Wild type
Chd4-/-
40
30
20
10
0
S
P
AI3
AI4
% of cell in each category/ 1 mm seminiferous tubule
60
40
20
0
S
P
AI3
AI4

Figure 5

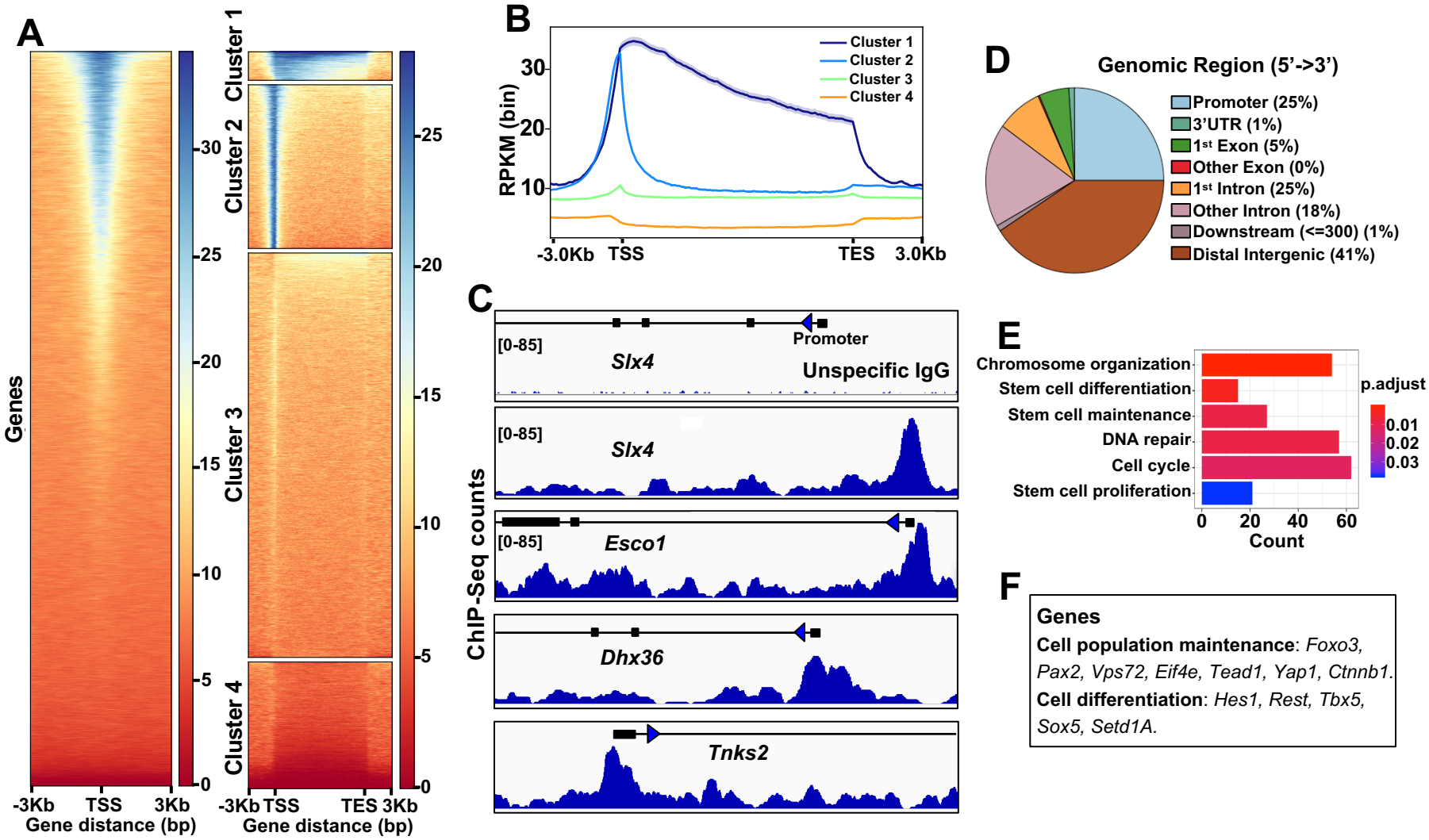
A
Genes
Cluster 1
Cluster 2
Cluster 3
Cluster 4
-3Kb TSS 3Kb
Gene distance (bp)
-3Kb TSS TES 3Kb
Gene distance (bp)
B
RPKM (bin)
Cluster 1
Cluster 2
Cluster 3
Cluster 4
-3.0Kb TSS TES 3.0Kb
C
ChIP-Seq counts
[0-85]
Slx4
Promoter
Unspecific IgG
[0-85]
Slx4
[0-85]
Esco1
Dhx36
Tnks2
D
Genomic Region (5'->3')
Promoter (25%)
3'UTR (1%)
1st Exon (5%)
Other Exon (0%)
1st Intron (25%)
Other Intron (18%)
Downstream (<=300) (1%)
Distal Intergenic (41%)
E
Chromosome organization
Stem cell differentiation
Stem cell maintenance
DNA repair
Cell cycle
Stem cell proliferation
p.adjust
0.01
0.02
0.03
0 20 40 60
Count
F
Genes
Cell population maintenance: Foxo3, Pax2, Vps72, Eif4e, Tead1, Yap1, Ctnnb1.
Cell differentiation: Hes1, Rest, Tbx5, Sox5, Setd1A.

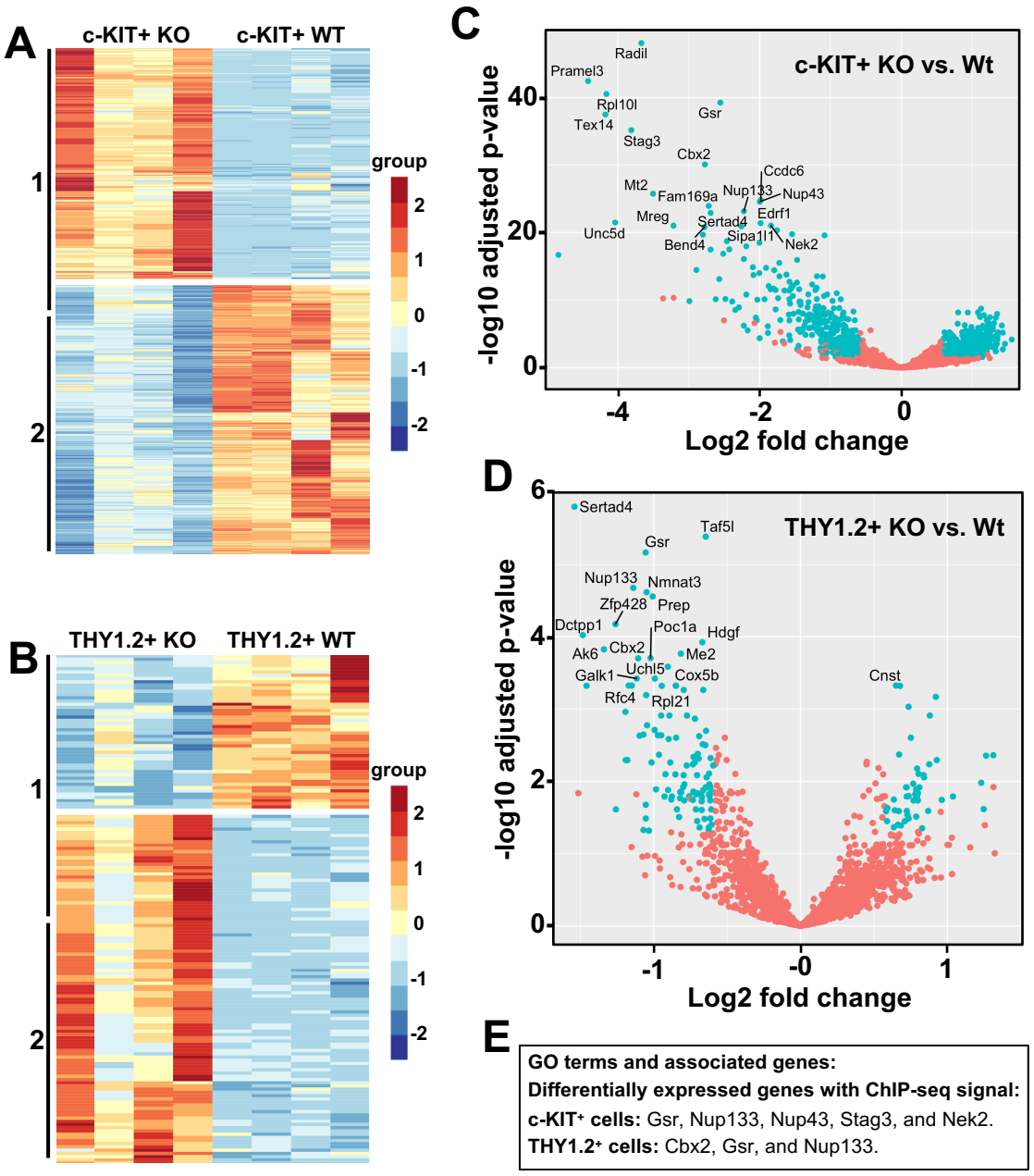
A
c-KIT+ KO
c-KIT+ WT
group
2
1
0
-1
-2
1
2
B
THY1.2+ KO
THY1.2+ WT
group
2
1
0
-1
-2
1
2
C
c-KIT+ KO vs. Wt
-log10 adjusted p-value
Log2 fold change
Radil
Pramel3
Rpl10l
Tex14
Gsr
Stag3
Cbx2
Ccdc6
Mt2
Fam169a
Nup133
Nup43
Mreg
Sertad4
Edrf1
Unc5d
Bend4
Sipa1l1
Nek2
40
20
0
-4
-2
0
D
THY1.2+ KO vs. Wt
-log10 adjusted p-value
Log2 fold change
Sertad4
Taf5l
Gsr
Nup133
Nmnat3
Zfp428
Prep
Dctpp1
Poc1a
Hdgf
Ak6
Cbx2
Me2
Galk1
Uchl5
Cox5b
Cnst
Rfc4
Rpl21
6
4
2
0
-1
-0
1
E
GO terms and associated genes:
Differentially expressed genes with ChIP-seq signal:
c-KIT+ cells: Gsr, Nup133, Nup43, Stag3, and Nek2.
THY1.2+ cells: Cbx2, Gsr, and Nup133.

Figure7

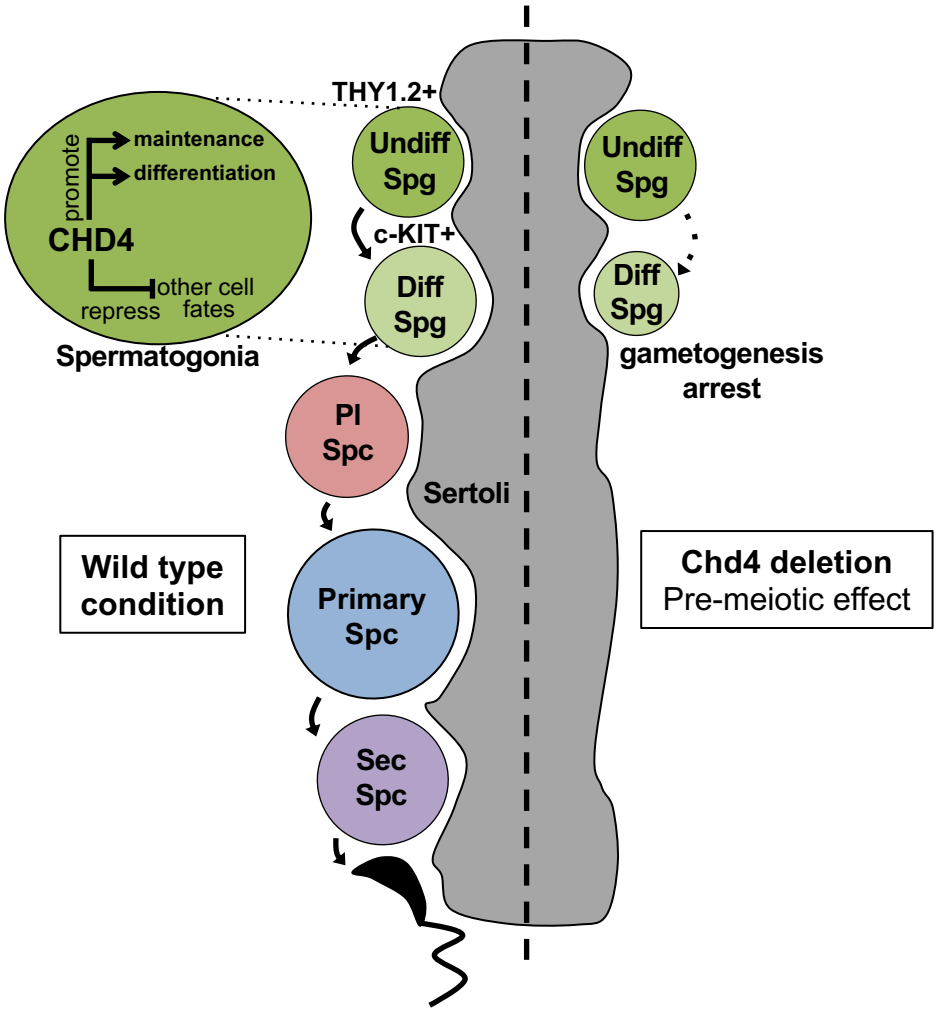
THY1.2+
promote
maintenance
differentiation
CHD4
repress
other cell fates
Spermatogonia
Undiff Spg
c-KIT+
Diff Spg
Undiff Spg
Diff Spg
gametogenesis arrest
Pl Spc
Sertoli
Primary Spc
Sec Spc
Wild type condition
Chd4 deletion
Pre-meiotic effect